Royal Aeronautical Society
5th Aircraft Structural Design Conference
Manchester, United Kingdom, 3-6 October 2016

SAFE-LIFE FATIGUE AND SENSITIVTY ANALYSIS: A PATHWAY TOWARDS EMBRACING UNCERTAINTY?

Joshua Hoole, Dr. Pia Sartor, Professor Jonathan Cooper

Department of Aerospace Engineering, University of Bristol, Queen's Building, University Walk, Bristol. BS8 1TR. UK.

ABSTRACT

Within the aerospace industry, conservatism exists within the safe-life fatigue design process of safety critical structures. This conservatism exists due to reduction factors which are required to counteract the probabilistic nature of fatigue and results in components that have to be retired from service prematurely. Understanding the sources of uncertainty and how they propagate from design inputs to the component safe-life is the first step to challenging the conservatism currently required. Variance Based Sensitivity Analysis (VBSA) can be used to apportion the uncertainty within a process output to the uncertainty within the process inputs. This paper explores the feasibility of applying VBSA methods to the safe-life design process using a landing gear case study and the "Sensitivity Analysis For Everybody" (SAFE) toolbox. The VBSA results identified that the parameter representing the number of cycles to failure associated with the cyclic load which accumulated the most fatigue damage within the component provided the largest contribution to the uncertainty within the component safe-life value. Whilst the over-arching concept of VBSA was found to be suitable for further application, the specific implementation presented within this paper displayed limitations, which are to be rectified if VBSA methods are to be applied within future work.

Keywords: Safe-life Fatigue, Variance Based Sensitivity Analysis, Uncertainty Quantification, SAFE Toolbox, Landing Gear

1. INTRODUCTION

Within the aerospace industry, many safety critical structural components are required to remain crack-free whilst in-service [1]. Cracks can initiate from static overloads as well as fatigue loading, which is composed of the cyclic loads that the component will be exposed to in-service. The cyclic loads carried by landing gear during taxi, take-off and landing are an example of fatigue loads [2]. The crack-free requirement exists for specific aerospace components where fatigue crack initiation and propagation may not be identified during routine maintenance inspections, or for components whose failure due to fatigue would be 'catastrophic' (i.e. resulting in the loss of the aircraft) [3]. Therefore, components which are manufactured using materials with short critical crack lengths, such as high-tensile steels [3], as well as single-load path structures [1], fall under the crack-free fatigue requirement. In order to ensure these components satisfy the crack-free requirement, a 'safe-life' must be defined for the component. A safe-life represents the number of load cycles that the component can sustain before removal from service to prevent catastrophic fatigue failure occurring [4]. Within the aerospace industry, a component safe-life is typically expressed as a maximum number of flight cycles or flight hours, beyond which, the component must be removed from service and retired or overhauled [5].

The safe-life fatigue design process is used to predict the safe-life for aerospace components such as landing gear structural components and elements of helicopter power transmissions. The safe-life fatigue design process is unique to the aerospace industry [6]. The core of the safe-life fatigue design process is based upon the prediction of the cyclic loads that the component will be exposed to in-service [4]. These loads are then coupled with fatigue design data based upon extensive experimental material testing to characterise how the number of load cycles to failure for the component material varies with the applied cyclic loads [3]. This material data is generated using material coupons that are representative of the component and an SN curve fit is then used to identify how the number of load cycles to failure varies with the magnitude of the applied cyclic stress [7].

Even though fatigue analysis is a critical element of ensuring safety critical structural components retain their integrity in-service, significant uncertainty exists within the inputs of the safe-life design process, due to fatigue being a complex and probabilistic phenomena [3]. The uncertainty contained within the process inputs has been attributed to the variability in the experimental material design data and the limitations of predicting the loads that the component will experience in-service [4]. In addition, a significant number of assumptions are required to conduct the safe-life design process, especially when considering the fatigue damage model used [7]. The uncertainty within the process inputs propagates through the design process, resulting in uncertainty within the predicted safe-life value for components [4]. As failure is unacceptable for safe-life components, reduction factors are applied to the experimental fatigue design data and overall predicted component safe-life [8]. In order to mitigate the uncertainty within the process, component safe-life values are reduced by a reduction factor of 3 to 5 depending on the amount of coupon and component testing performed [8][9].

The application of reduction factors results in a potentially conservative approach to safe-life fatigue design. This often results in components being removed from service prematurely in order to be overhauled or retired [10], increasing aircraft maintenance costs. In addition, such conservatism within design can result in heavier components [11]. On the other hand, safe-life components have been shown to fail prematurely in-service due to the assumptions made within the current design process failing to account for effects resulting from material defects, component corrosion and overloads [12]. Therefore, a challenge of the conservatism currently applied to component safe-life values is required to support the development of more efficient components which are still safe and reliable in-service.

The first step in challenging the conservatism within the safe-life design process is to understand the sources of uncertainty within the process and how they propagate from the process inputs to the predicted component safe-life value. Through generating insight and understanding into the extent to which specific areas of uncertainty contribute towards the uncertainty within component safe-life values, future work can be focused on those areas which have the greatest impact on the overall process uncertainty. This future work could support a reduction in the conservatism currently required within the process. Future work could also support the development of a probabilistic analysis method to better represent the probabilistic nature of fatigue, aligning fatigue analysis with the 'probability of failure' approach used for aircraft systems [8].

Variance Based Sensitivity Analysis (VBSA) methods have been proposed as statistical techniques which apportion the uncertainty in the output of a process to the different sources of uncertainty within the process input [13] [14]. VBSA methods are an extension of traditional sensitivity analysis methods which study how a process output changes with variations in the process input and are based upon quantifying the uncertainty in the process inputs as probability distributions [15]. The process output is then evaluated over a large number of iterations, each time randomly sampling values for each input parameter from its respective probability distribution [15]. VBSA methods can then be applied to evaluate how the variance of the output of the process varies with the differing input values. Therefore, VBSA methods are able to identify the uncertain parameters which provide the greatest contribution to the output uncertainty [16]. This produces a parameter 'ranking', which orders each process parameter with respect to the size of its individual contribution to the output uncertainty [14]. This ranking can be used to focus future work to target a reduction of the uncertainty contained within influential parameters [13].

VBSA methods are known as 'global' sensitivity analysis methods as they enable all process parameters to be varied at the same time and therefore, provide sensitivity analysis across the entire potential input space of the process [14]. As a result, VBSA methods are able to evaluate non-linear models and processes. Because of this ability, VBSA methods have been applied across numerous fields, including environmental modelling [17], the design of transportation systems [18] and in the aerospace industry, concerning the optimisation of a rocket launcher design [19]. Due to the wide applicability of VBSA methods, 'toolboxes' have been developed to enable researchers to apply such methods to their projects with ease [17] [20]. One example of such a toolbox is the 'Sensitivity Analysis For Everybody' (SAFE) Matlab toolbox developed by the Department of Civil Engineering at the University of Bristol [20].

VBSA methods have already been applied to a limited extent to the safe-life fatigue analysis of rotorcraft components. Ref [22] provides a case study of the American Helicopter Society's 'Round Robin' helicopter fatigue problem, within which the magnitude of the applied loads and elements of the fatigue design data were modelled as probability distributions. VBSA methods were then used to identify the parameter which contributed most to the uncertainty in the safe-life value for the component [22]. Whilst Ref [22] supports the view that the ranking of uncertain parameters will support the development of future work to challenge the conservatism currently required within the safe-life fatigue design process, only a limited number of uncertain parameters were considered. The VBSA did not account for the uncertainty resulting from assumptions made within the process and was limited to the magnitude of the applied loads and the parameters used for the SN curve 'fit' of the experimental fatigue data. Within the wider literature, variability in the number of cycles to failure at a given stress for a material has been modelled using probability distributions fitted to the data points generated during material coupon testing [23] [24]. In addition, the variability in the number of applied cycles of a given load has also been modelled as a probability distribution within the development of a probabilistic approach to the fatigue of metallic lugs [25]. However, these distributions have not been used to support the application of VBSA methods to the safe-life design process. Therefore, a VBSA study which incorporates further and more complete modelling of the uncertainty contained within parameters throughout the process is required. Finally, it should be noted that the application of VBSA methods in Ref [22] was limited to the safe-life fatigue analysis of rotorcraft components. The application of VBSA methods to the fatigue design of a landing gear component is yet to be performed. Landing gear represent a very different safe-life design case due to their significantly lower number of loading cycles per flight when compared to rotorcraft components.

The safe-life fatigue design process presents a challenge regarding the application of VBSA methods as the process contains a large number of uncertain parameters, which can result in significant computational expense when implementing VBSA techniques [14]. In addition, visualisation of results is a vital part of sensitivity analysis to ensure intuitive and clear understanding of the analysis results [20], especially to those without a deep statistical

background. As the number of uncertain parameters increases, the ease of interpreting visualisation methods reduces [26] [27]. Therefore, a feasibility study is required to assess the suitability of applying VBSA to the safe-life design process in future work.

In order to build upon the current state-of-the-art within the literature, this paper will develop a landing gear component fatigue design case study in order to assess the feasibility of applying VBSA methods to the safe-life fatigue design process using the SAFE toolbox. This will be achieved by developing a sensitivity analysis framework and producing a mathematical model of the safe-life design process. Comprehensive modelling of the uncertain parameters as probability distributions within the process will also be performed in order produce a ranking of the parameters with respect to their contribution to the uncertainty within the component safe-life value. A novel visualisation technique will also be presented in order to clearly identify the individual parameter contributions to the uncertainty in the component safe-life value.

2. METHODOLOGY

2.1. Introduction to Methodology and Analysis Framework

This section of the paper introduces the methodology used to apply VBSA methods to the safe-life fatigue design process, including the safe-life fatigue design process model, uncertainty quantification process and VBSA method implemented within this paper. The analysis framework developed to conduct VBSA of the safe-life design process is shown in ***Fig. 1***. Similar frameworks have been reported within the literature [14] [15] and this shows the versatility and generalised nature of application of VBSA methods. The remainder of the methodology section of this paper follows the flow of the framework and describes how each step was executed. The steps in ***Fig 1.*** are as follows:

1) **Safe-Life Fatigue Design Process** – In order to conduct sensitivity analysis of a process, the process itself must first be thoroughly understood. This includes the identification of the parameters (e.g. material properties) and mathematical functions used within the process.
2) **Process Model** – The process must then be converted into a mathematical model comprising of the parameters and functions identified within Step 1. This results in the process output (e.g. the component safe-life value) being the result of evaluating a function comprised of the input parameters of the process.
3) **Uncertainty Quantification** – The parameters which are known to be uncertain are modelled as probability distributions (e.g. Gaussian, Weibull, Uniform etc.) based upon existing data sets [14] [16].
4) **VBSA Method** - The VBSA method is applied to the process using the SAFE toolbox. This includes the sampling methods used to sample values from the input parameter probability distributions.
5) **Parameter Ranking –** The output of the VBSA is the ranking of the parameters with respect to their contribution to the uncertainty in the component safe-life value. These results can also be visualised to support the intuitive understanding of the analysis results. The VBSA results are validated by comparing the parameter ranking with the results of an alternative Global Sensitivity Analysis (GSA) method.
6) **Future Work** – The VBSA results can be used to focus future work at the parameter(s) which contribute most the uncertainty in the component safe-life value.

2.2. Safe-Life Fatigue Design Process

The safe-life fatigue design process is visualised as a flowchart overleaf in ***Fig. 2*** and is composed of three distinct phases: *fatigue design data*, *fatigue loading* and the *fatigue damage model*.

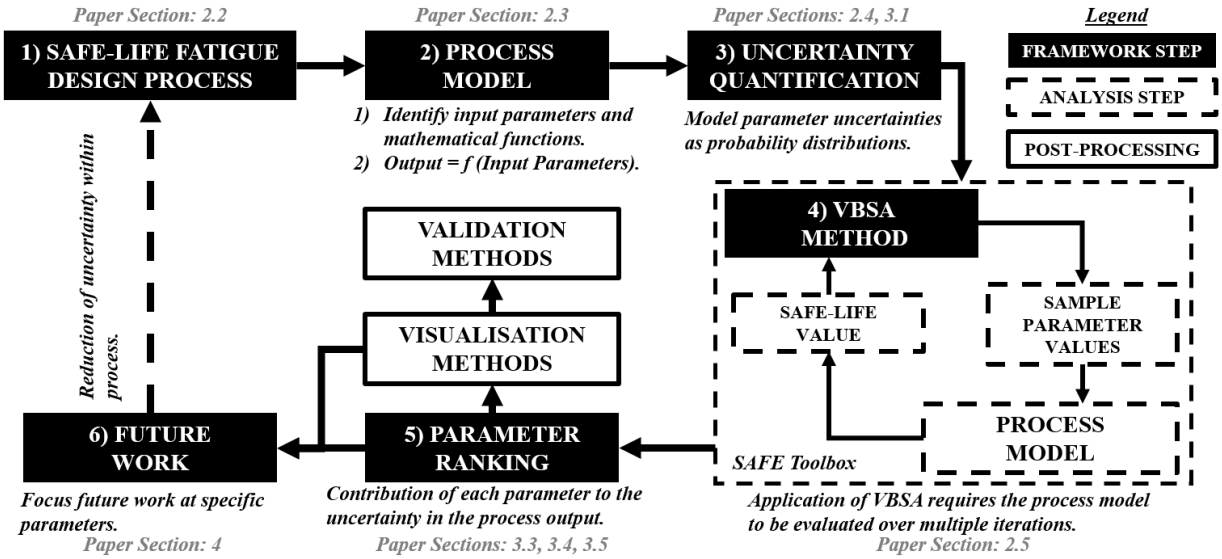

Figure 1: *Analysis framework for implementing Variance-Based Sensitivity Analysis (VBSA).*

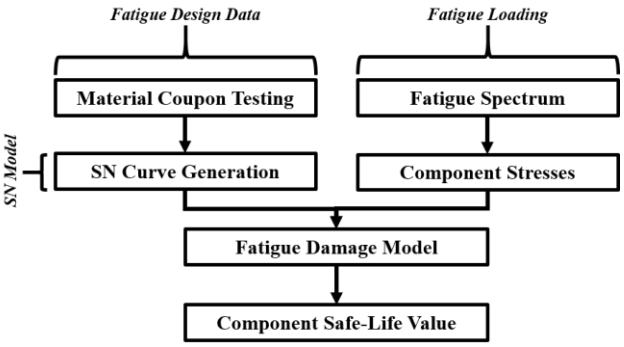

Figure 2: *Safe-life Design Process.*

The first stage of the safe-life design process is the generation of fatigue design data for the material to be used within the component. This design data establishes the fatigue 'response' of the material and this is defined as how the number of load cycles to cause fatigue failure varies with the applied cyclic stress [7]. This data is generated experimentally by applying uniaxial cyclic stresses of $\pm\sigma$ stress magnitude with a zero mean stress (known as a fully reversed stress) to material coupons until each coupon fails [7]. These coupons incorporate key features of the component geometry and therefore can include notches, holes and any material/surface treatments that are to be included within the component [28]. The cyclic loading is repeated at various stress magnitudes and the number of cycles to failure is recorded for each stress magnitude. An 'SN curve' can then be fitted to the data which represents how the number of applied stress cycles to cause failure (N) varies with the applied cyclic stress (S). This allows the number of cycles to cause fatigue failure (N_{fail}) to be found for any applied cyclic stress magnitude. An example of an SN curve for a 4340 steel is shown in ***Fig. 3*** [29].

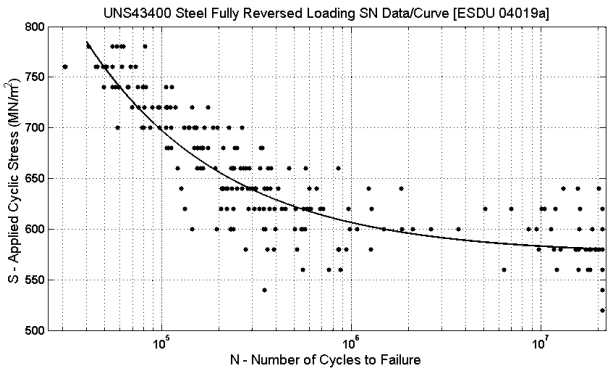

Figure 3: *4340 Steel SN curve and data, after Ref [29].*

The next stage of the safe-life design process is to predict the cyclic stresses that the component will be exposed to in-service. Fatigue spectra are a representation of the maximum (i.e. tension) and minimum (i.e. compressive) cyclic load levels that a component will be exposed to in-service. These are sourced from standardised fatigue spectra (such as the HELIX spectrum for rotorcraft components [30]), or developed from measurements of in-service loads using methods such as 'rainflow counting' [31]. An example fatigue spectra is shown overleaf in ***Fig. 4*** and shows the peak load value against the 'exceedance' for each peak load, which represents how often a given load level is exceeded within the fatigue spectrum [31]. The complete fatigue spectrum is known as a 'loading cycle' and within the aerospace industry typically represents the cyclic loading across a number of flights [31].

The fatigue spectrum is then discretised into 'i' load blocks which each represent a cyclic load that is applied to the component as shown in ***Fig. 4***. Load blocks are typically generated arbitrarily, by dividing the spectra into blocks of equal exceedance value [31]. Therefore, the resulting load blocks are composed of maximum and minimum load levels which may not actually occur together in-service [4]. These load levels are then converted to cyclic stress levels σ_{MAX_i} and σ_{MIN_i} based upon the component geometry, typically using Finite Element software [32]. The cyclic stress levels are transformed into individual cyclic stresses comprised of a stress amplitude (σ_{a_i}) and a mean stress (σ_{m_i}) using ***Equations 1*** and ***2*** respectively [33]. Each load block is also defined by the number of stress cycles that are applied (n_i). The number of applied cycles for each load block is computed as the difference between the maximum and minimum exceedance values for each load block [31].

$$\sigma_{a_i} = \frac{\left(\sigma_{MAX_i} - \sigma_{MIN_i}\right)}{2} \quad (1) \qquad \sigma_{m_i} = \frac{\left(\sigma_{MAX_i} + \sigma_{MIN_i}\right)}{2} \quad (2)$$

The load block stresses are then converted into zero-mean 'fully reversed' stresses (σ_i) in order to be consistent with the SN curves generated for the component material. This is achieved using a 'constant-life model', an example of which is the Goodman Model [28] shown in ***Equation 3***, where σ_{UTS} is the ultimate tensile strength of the material.

$$\sigma_i = \frac{\sigma_{a_i}}{\left[1 - \left(\frac{\sigma_{m_i}}{\sigma_{UTS}}\right)\right]} \quad (3)$$

The application of the Goodman Constant-Life Model results in each load block being defined by the cyclic stress magnitude (σ_i) and the number of cycles that the cyclic stress is applied for (n_i).

The final stage of the safe-life fatigue design process combines the fatigue loading cycle with the material SN curve using a fatigue damage model. This computes the fatigue damage accumulated within the component for each load block. Miner's Rule, as shown in ***Equation 4***, is used as the safe-life fatigue damage model within the aerospace industry due to its simplicity and applicability across many different component types [3] [7].

$$D_{cycle} = \sum_{i=1}^{i_{tot}} \frac{n_i}{N_{fail_i}} \quad (4)$$

Within Miner's rule, n_i is the number of applied cycles for a given stress σ_i from load block 'i' and N_{fail_i} is the number of cycles to cause failure sourced from the SN curve for the same stress σ_i. 'i_{tot}' is the total number of load blocks. The ratio of $\frac{n_i}{N_{fail_i}}$ is computed for each load

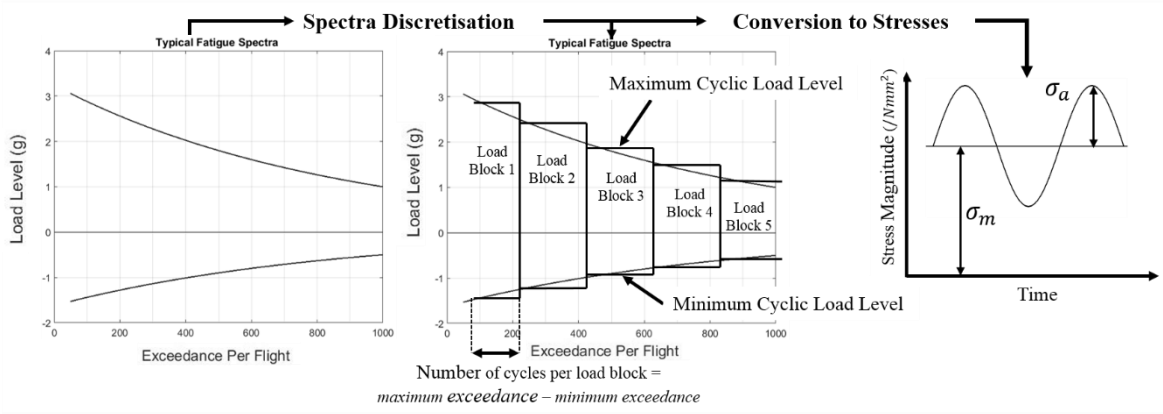

Figure 4: *Generation of cyclic stresses from the fatigue loading spectrum.*

block and these are summated to calculate the fatigue damage accumulated per loading cycle 'D_{cycle}'. It should be noted that some materials, such as high tensile steels exhibit a 'fatigue limit' (σ_{FL}), which defines a cyclic stress level below which the component can be cyclically loaded indefinitely without failure [33]. Therefore, Miner's Rule assumes that load blocks with stress magnitudes below the fatigue limit do not contribute to the fatigue damage accumulated within the component [7]. Component fatigue failure is assumed to occur when $D_{cycle} = 1$, as this represents that all of the available fatigue life within the component has been consumed. Hence, the failure criterion for Miner's Rule is therefore $D_{fail} = 1$ [3]. Finally, the component safe-life is computed using ***Equation 5*** [3] [7].

$$Safe-life = \frac{Damage\ value\ to\ cause\ failure}{Damage\ accumulated\ per\ loading\ cycle} = \frac{D_{fail}}{\sum \frac{n_i}{N_{fail_i}}} = \frac{D_{fail}}{D_{cycle}} \quad (5)$$

2.3. Landing Gear Component Case Study and Process Model

A hypothetical safe-life case study was required in order for VBSA to perform ranking of the parameters within the safe-life fatigue design process of a landing gear component. This required the selection of material SN data and the identification of a landing gear component fatigue spectrum from the literature. The material for the component was selected to be 300M steel. 300M steel is a low carbon alloy steel used for landing gear structures due to its high-tensile strength and ductility, which are required due to the high static loads carried by landing gear [34]. MIL-HDBK-5H provides a fully reversed SN curve and data for 300M steel and is reproduced in ***Fig. 5*** [35]. 300M steel has an ultimate tensile strength of σ_{UTS} = 1930 N/mm^2 [35] and a fatigue limit of σ_{FL} = 138 N/mm^2 [35].

The fatigue spectrum for the case study was reproduced from the landing gear fatigue spectrum of an US Navy F-4J fighter aircraft [36] shown in ***Fig. 6***. This spectrum shows the stress levels carried within the F-4J landing gear across a series of 8,000 landings. As Ref [36] is a stress spectrum, the definition of a component geometry was not required. Ref [36] identifies that the stresses were sourced from a structural component of the main landing gear and this was assumed to be the landing gear main fitting. The spectrum was discretised into 18 load blocks as shown in ***Fig. 6***. The stress levels for each load block were converted into fully reversed stresses (σ_i) using ***Equations 1-3*** to provide 'nominal' stresses and are shown overleaf in ***Table 1***. The fatigue design case study presented above was then converted into a Matlab model which computed the component safe-life value using ***Equations 1-5***. From applying Miner's Rule to the F-4J spectrum and 300M SN data, the component safe-life value was found to be **23,569 landings**. The Matlab model enabled the safe-life value output 'Y' could be expressed as a mathematical function of the input parameters as shown in ***Equation 6***.

$$\text{Safe Life} = Y = f\left(\sigma_{MAX_{1\ to\ 18}}, \sigma_{MIN_{1\ to\ 18}}, n_{1\ to\ 18}, N_{fail_{1\ to\ 18}}, \sigma_{UTS}, \sigma_{FL}, D_{fail}\right) \quad (6)$$

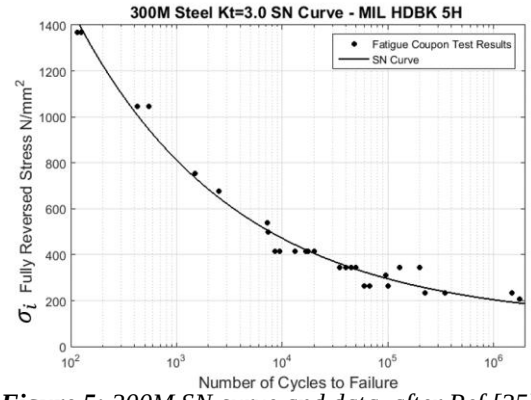

Figure 5: *300M SN curve and data, after Ref [35].*

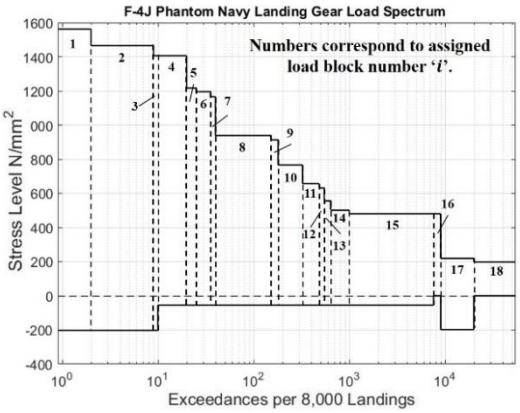

Figure 6: *F-4J Landing Gear Fatigue Spectrum, after Ref [36].*

Table 1: *Cyclic load blocks for the discretised F-4J landing gear fatigue spectrum.*

Load Block, i	σ_{MAX_i} N/mm^2	σ_{MIN_i} N/mm^2	Exceedances per 8000 Landings	$\boldsymbol{\sigma_i}$ $\boldsymbol{N/mm^2}$	$\boldsymbol{n_i}$
1	1563	-202	2	**1364**	**2**
2	1465	-202	9	**1239**	**7**
3	1404	-202	10	**1166**	**1**
4	1404	-54	20	**1121**	**10**
5	1219	-54	25	**912**	**5**
6	1198	-54	35	**889**	**10**
7	1165	-54	40	**856**	**5**
8	940	-54	150	**645**	**110**
9	912	-54	180	**621**	**30**
10	764	-54	325	**502**	**145**
11	656	-54	485	**421**	**160**
12	633	-54	545	**404**	**60**
13	558	-54	640	**352**	**95**
14	502	-54	1000	**315**	**360**
15	481	-54	7600	**301**	**6600**
16	481	0	9000	**275**	**1400**
17	218	-197	20000	**12**	**11000**
18	197	0	54284	**104**	**34284**

2.4. Uncertainty Quantification Process

From developing the Matlab programme, the total number of parameters 'k' within the model was identified to be $k = 75$; 18 σ_{MAX_i} (i.e. one for each load block), 18 σ_{MIN_i}, 18 n_i, 18 N_{fail_i}, σ_{UTS}, σ_{FL} and D_{fail}. The 'i' subscript identifies the load block that each parameter belongs to (e.g. σ_{MAX_2} is the maximum stress level for load block 2). Where there are multiple parameters of the same type, such as the 18 N_{fail_i} parameters, these can be grouped into a single parameter 'family'. Uncertainty exists within each of these parameter families and can arise from **aleatoric** uncertainty (i.e. 'randomness' or variability within parameters) or through **epistemic** uncertainty (i.e. the assumptions made during the analysis) [16].

Uncertainty is present within the load block stress level parameters σ_{MAX_i} and σ_{MIN_i} as it is not possible for the predicted loads to fully capture the range of load magnitudes that components will experience in-service [4]. In addition, uncertainty is also introduced by the discretisation of the fatigue spectrum. In order to capture all of the loads from the spectrum, an infinite number of load blocks would be required and this is infeasible in practice [31]. Due to discretisation, each load block could have a range of potential load levels as shown in ***Fig. 7***.

Uncertainty is also experienced within the number of cycles that each load block is applied for n_i. The uncertainty within n_i arises due to factors which vary with every flight such as aircraft weight and landing attitude [37]. Therefore, the number of load cycles generated for each load block may not be representative of the number of load cycles that the component will be exposed to in-service.

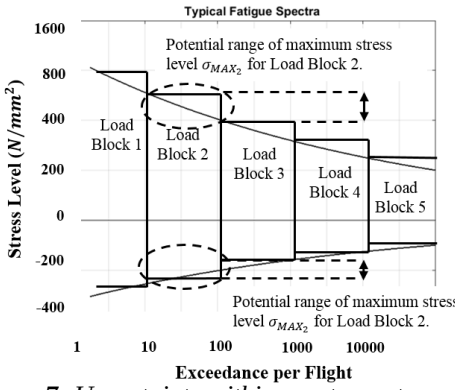

Figure 7: *Uncertainty within spectrum stress levels.*

The uncertainty in the N_{fail_i} parameter family exists due to variability in the material used within the coupon tests in the form of material defects and is known known as SN data 'scatter' (Note the data points on ***Fig. 5***) [28]. The scatter, and hence uncertainty, in N_{fail_i} increases as the applied cyclic stress reduces [28]. Uncertainty also exits due to the curve-fitting methods used across the industry, which vary significantly between manufacturers [38]. Material variability within test coupons also results in uncertainty within the ultimate tensile strength σ_{UTS} [39] and fatigue limit σ_{FL} [22] of 300M steel.

Uncertainty within the Miner's Rule failure criterion D_{fail} exists due to assumptions made within the Miner's Rule fatigue damage model. One assumption is that fatigue damage is independent of any previous damage accumulated [7]. However, as fatigue damage is in the form of ever increasing material defects which interact with one another, this assumption is contradicted [40]. In addition, the effect of loading sequence is neglected by Miner's Rule. It has been shown that a low to high stress loading sequence results in longer fatigue lives, whilst high to low stress loading sequences results in shorter fatigue lives [7].

Therefore, in-service components may fail at a value of D_{cycle} which is greater than or less than 1 [7], resulting in uncertainty within the Miner's Rule failure criterion D_{fail}.

In order to quantify the uncertainty within each parameter of the safe-life design process, Matlab was used to fit probability distributions (e.g. Gaussian, Weibull, Uniform etc.) to publically available data using distribution types which have been presented within the literature. The resulting distributions are presented and discussed within the '*Results and Discussion'* section of this paper.

2.5. VBSA Method: Sampling and Sensitivity Indices

A VBSA method was used to produce the parameter ranking in order to identify the parameters which provide the greatest contribution to the uncertainty within the safe-life value of the landing gear component. This was achieved by using statistical processes implemented by the SAFE toolbox [20]. In order to generate the parameter ranking, 'sensitivity indices' are computed which measure the contribution of an individual input parameter to the variance in the process output [14]. The VBSA sensitivity index computed by the SAFE toolbox is known as the 'main effect' or 'first order index' S_{I_j} [20].The main effect of a parameter can be defined as the reduction in the output variance that is obtained when the parameter is fixed to a specific value [14]. As a result, a parameter with a larger S_{I_j} value will provide a greater reduction in the output variance when fixed and therefore, provides a greater contribution towards the uncertainty in the process output.

The main effect S_{I_j} of parameter 'x_j' is computed using ***Equation 7*** [14], where; $V(Y)$ is the variance in the process output Y, $Y|x_j$ is the output value Y when parameter x_j is fixed to a specific value, $x_{\sim j}$ denotes all parameters excluding x_j, $E_{\boldsymbol{x}_{\sim j}}(Y|x_j)$ is the mean value of $Y|x_j$ taken over all parameters excluding parameter x_j and $V_{x_j}(z)$ is the variance of the argument z taken over all possible values of parameter x_j [41]. For clarity, the numerator of ***Equation 7*** can be interpreted as the expected reduction in the variance of the model output that would be obtained if parameter x_j could be fixed to a known value [41].

$$S_{I_j} = \frac{V_{x_j}(E_{\boldsymbol{x}_{\sim j}}(Y|x_j))}{V(Y)} \qquad (7)$$

'Total effects' can also be computed, which account for the parameter main effect and any interactions with the other parameters within the process [14]. Whilst also calculated by the SAFE toolbox, main effects were only considered as these indices are often used for parameter ranking [14].

The first stage of computing the main effect index in ***Equation 7*** uses Latin Hypercube Sampling (LHS) to sample one value from each parameter probability distribution for 'N' iterations. Each iteration represents one set of complete input values for the process. LHS is a sampling method which divides the probability distributions for each parameter into regions of equal probability [42].The use of LHS ensures that each region of the parameter probability distributions is represented in the final sample set for each parameter [42]. This results in an input matrix $\bar{X}$ where each column 'j' contains the sampled values of an individual parameter for 'N' rows (i.e. each row 'l' represents one sampling iteration).

In order to reduce the computational cost of evaluating the main effect indices, the SAFE toolbox uses an estimator to compute the numerator of the main effect index [41]. The estimator requires the input matrix $\bar{X}$ to be divided and resampled into additional input matrices. $\overline{X_A}$ is the first $\frac{N}{2}$ rows of $\bar{X}$ (i.e. the upper 'half' of the original input matrix) and $\overline{X_B}$ is the latter $\frac{N}{2}$ rows of $\bar{X}$. A matrix $\overline{X_C^j}$ is generated for each of the 'x_j' parameters. Within each $\overline{X_C^j}$ matrix, column 'j' of the matrix is sourced from matrix $\overline{X_A}$ and the rest of the columns are sourced from $\overline{X_B}$. The estimator used is shown in ***Equation 8*** [41], where $f(\overline{X_A})_l$ and $f(\overline{X_C^j})_l$ are the output value of the process model when using row 'l' of the $\overline{X_A}$ matrix and $\overline{X_C^j}$ matrix as input parameter values respectively. f_0 is the mean of the output when using input parameter values from $\overline{X_A}$ across all 'N' iterations. This estimator is summed for all 'N' iterations and repeated separately for each parameter. This process is visualised as a flowchart in ***Fig. 8***. The evaluation of the estimator in ***Equation 8*** provides the main effect S_{I_j} values for each parameter x_j and therefore permits the ranking of parameters.

$$V_{x_j}\left(E_{x_{\sim j}}(Y|x_j)\right) = \frac{1}{N}\sum_{l=1}^{N} f(\overline{X_A})_l \; f(\overline{X_C^j})_l - f_0^2 \qquad (8)$$

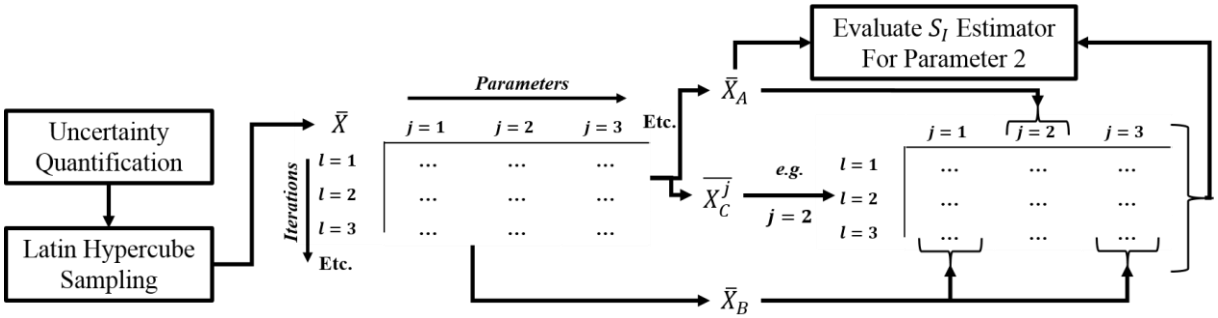

Figure 8: *Visualisation of the estimator calculation process for the main effect sensitivity index.*

3. RESULTS AND DISCUSSION

This section of the report presents and discusses the results from the application of the VBSA framework and methodology to the landing gear component case study.

3.1. Uncertainty Quantification of the Safe-Life Design Process

Uncertainty quantification was performed for each of the process parameters. Due to the large number of parameters, only a few examples of the distributions for each of the parameter families are shown.

In order to quantify the uncertainty in σ_{MAX_i} and σ_{MIN_i} uniform probability distributions were generated between the maximum and minimum possible stress levels from the load spectrum. Uniform distributions were selected to represent the interval value nature of the stress levels resulting from load spectrum discretisation [43]. Examples of the uniform distribution ranges are shown in ***Table 2***.

Table 2: *Example uniform distributions for σ_{MAX_i} and σ_{MIN_i}* parameter families.

Load Block	σ_{MAX_i} Range	σ_{MIN_i} Range
5	[1198, 1219]	[-202, -54]
10	[656, 764]	[-202, -54]
15	[481, 502]	[-202, -54]

The uncertainty within the n_i parameter family was quantified using fatigue load measurements from the DH112 'Venom' Jet Fighter [37]. This study measured the number of cycles for specific cyclic load magnitudes on the DH112 landing gear due to variations in aircraft weight, touchdown rate and landing speed. The scatter in the number of cycles for the specific cyclic load magnitude from Ref [37] is shown in ***Fig. 9***. As Ref [37] considered various landing conditions, the scatter in the number of applied load cycles was considered to be a suitable proxy for the variability in n_i across the landing gear component loading spectrum. A log-normal distribution was required in order account for the skewed distribution of the data points and is shown on ***Fig. 9***.

Log-normal distributions are defined by two parameters, μ and σ^{LN} which represent the mean and variance of the parameter's natural logarithm respectively. As n_i was a family of 18 parameters, the distribution was required to be generalised across all of the load blocks. From Ref [37] it was found that the maximum number of load cycles was 3.2 times greater than the mean number of applied cycles and the minimum number of load cycles was 15.5 times smaller than the mean number of applied cycles. Therefore, for each n_i, the log-normal distribution was scaled such that the distribution was bounded by these maximum and minimum values, where the 'mean' number of applied cycles for each load block was the n_i value from ***Table 1.*** This resulted in a constant σ^{LN} distribution parameter for the family. ***Table 3*** shows examples of these scaled probability distributions.

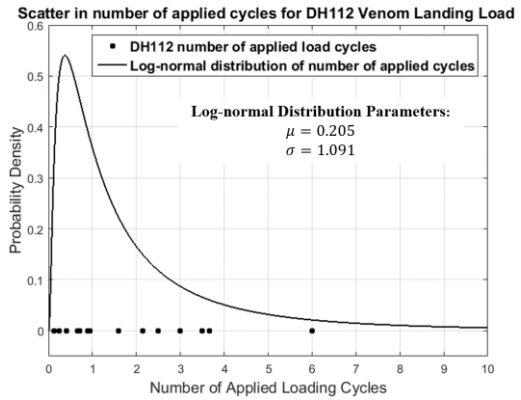

Figure 9: *Log-normal distribution for n_i.*

Table 3: *Example log-normal distribution parameters for the n_i family.*

Load Block	n_i Distribution μ	n_i Distribution σ^{LN}
5	1.63	0.30
10	5.00	0.30
15	8.18	0.30

Quantification of the uncertainty within the N_{fail_i} parameter was achieved using the 300M SN data [35] which provided data points for each stress level used to generate the SN curve. A log-normal distribution was fitted to the data points at each stress level. Log-normal distributions were used as it has been widely reported in the literature that coupon fatigue lives are typically log-normally distributed [23] [24]. It was found that the σ^{LN} distribution parameter increased as the cyclic stress magnitude was reduced (i.e. the 'scatter' within the number of cycles to failure increased as the cyclic stress magnitude decreased). Therefore, in order for the N_{fail_i} distribution for each load block to be generated accounting for the evolving distribution parameters, the μ and σ^{LN} values for each data set were plotted against the cyclic stress level σ_i associated with each data set and are shown in ***Fig. 10*** and ***Fig. 11*** respectively. Curve fits were then applied to each plot to enable μ and σ^{LN} to be computed for any applied stress. Therefore, a log-normal N_{fail_i} distribution could be generated for each load block. These double exponential curve fits are shown on ***Fig. 10*** and ***Fig. 11.*** The R^2

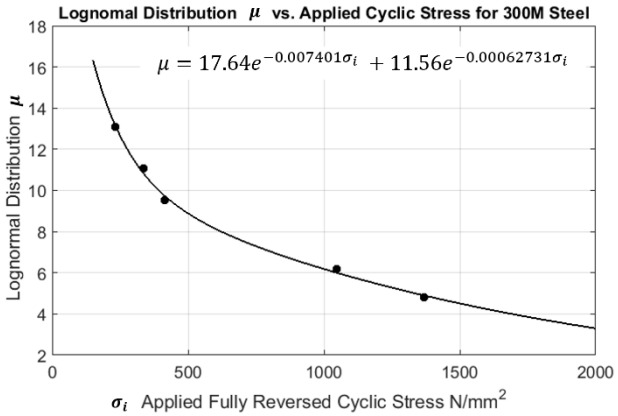

Figure 10: *N_{fail_i} Log-normal distribution μ vs σ_i.*

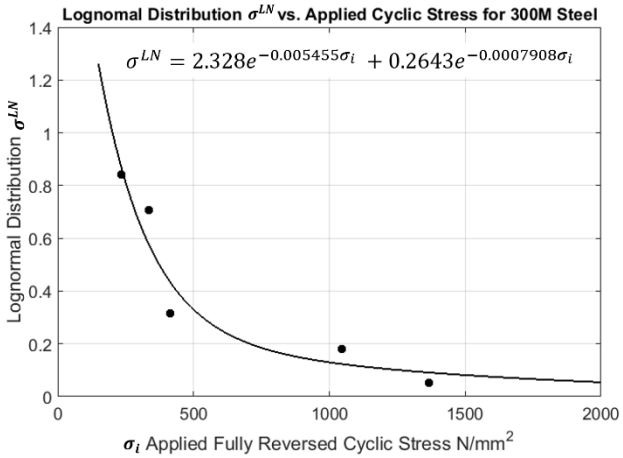

Figure 11: *N_{fail_i} Log-normal distribution σ^{LN} vs σ_i.*

'goodness of fit' values were 0.988 and 0.921 for the μ and σ^{LN} curves respectively (where $R^2 = 1$ represents a perfect curve fit). Examples of the resulting log-normal distribution parameters are shown in ***Table 4***.

Table 4: *Example N_{fail_i} log-normal distribution parameters.*

Load Block	Cyclic Stress σ_i N/mm^2	N_{fail_i} Distribution μ	N_{fail_i} Distribution σ^{LN}
5	912	6.54	0.14
10	502	8.87	0.33
15	301	11.47	0.66

Within the literature, Gaussian probability distributions have been used to represent the variability in the σ_{UTS} of high strength low alloy steels [39]. Therefore, the Gaussian probability distribution for 300M σ_{UTS} was generated using a mean and standard deviation based on the MIL-HDBK-5H 300M σ_{UTS} specification range for aerospace components of 1890 to 2000 N/mm^2 [35]. This resulted in a Gaussian distribution with a mean of 1945 N/mm^2 and a standard deviation of 78.5 as shown in ***Table 5***.

Uncertainty in σ_{FL} has also been quantified using a Gaussian probability distribution within the literature [22]. However, there was insufficient data to quantify the standard deviation of σ_{FL} within the 300M SN data. Hence, SN data for 4340 Steel (300M steel is a variant of this steel [2]) [29] was used to identify a typical standard deviation of the fatigue limit for high tensile steels and this was found to be σ_{sd} = 23.7. Using σ_{sd} and σ_{FL} = 138 N/mm^2. The distribution parameters are also shown ***Table 5***.

Table 5: *σ_{UTS} and σ_{FL} distribution parameters.*

Parameter	Distribution Type	Mean	Std. Dev.
σ_{UTS}	Gaussian	1945 N/mm^2	78.5
σ_{FL}	Gaussian	138 N/mm^2	23.7

Finally, experimental evidence has shown that for 4340 steel (equivalent results for 300M steel were not available) that a high to low (HL) stress sequence results in D_{fail} = 0.73 and a low to high (LH) stress sequence results in D_{fail} = 1.14 [44]. Due to the discretisation of the fatigue spectra, the order of loading is neglected and therefore, D_{fail} could vary between these values for a component in-service. In order to represent this 'bounded' behaviour, a Weibull distribution was used. The distribution parameters are shown in ***Fig. 12***, resulting in a distribution about the nominal value of $D_{fail} = 1$ and bounded between the HL and LH D_{fail} values. This resulted in a Weibull distribution defined by the parameters a = 1 and b = 20, which represent the 'mean' and 'spread' of the distribution.

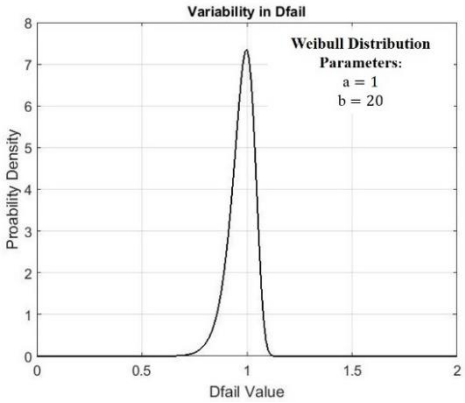

Figure 12: *D_{fail}* Weibull Distribution.

3.2. Implementation of the Safe-Life Fatigue Model and SAFE Toolbox

The LHS and main effect estimator (***Equation 8***) implemented by the SAFE Toolbox assumes uncertainty independence exists between the parameters [41]. Uncertainty independence infers that the probability distribution parameters of one process parameter are not governed by the uncertainty present within another parameter [45]. Violation of this assumption can result in incorrect parameter rankings as the uncertainty contribution of a dependent parameter cannot be distinguished from the uncertainty contribution resulting from the uncertain parameter used to generate the dependent parameter's probability distribution [45].

Within the safe-life fatigue design model, the probability distribution parameters for the number of cycles to failure parameter family N_{fail_i} are dependent on the magnitude of the applied cyclic stress σ_i as shown in ***Fig. 10*** and ***11***. As σ_i is generated from σ_{MAX_i}, σ_{MIN_i} and σ_{UTS}, all of which are uncertain parameters, a dependency exists between the uncertainty within N_{fail_i} and the uncertainty within the three stress parameter families. Therefore, the independent uncertainty assumption was violated. In order for the SAFE toolbox main effect method to be applied to the safe-life fatigue design process, the process was decomposed into two individual sub-models and VBSA studies (Note the 'SN Model' label on ***Fig 2***.):

1) **300M SN Model** - which investigates how the uncertainty in N_{fail_i} is attributed to σ_{MAX_i}, σ_{MIN_i} and σ_{UTS} using ***Equations 1-3*** and the curve fits for the N_{fail_i} log-normal distribution parameters.

2) **Fatigue Damage Model** - which investigates how the uncertainty in the landing gear component safe-life value is apportioned to N_{fail_i}, n_i, σ_{FL} and D_{fail} using ***Equations 4*** and ***5***.

By dividing the safe-life model into these two sub-models, the dependency between the uncertainty in N_{fail_i} and the σ_{MAX_i}, σ_{MIN_i} and σ_{UTS} stress parameters was de-coupled.

The 300M SN Model was also used to update the distribution parameters of the N_{fail_i} parameter family. This was required to represent the increase in uncertainty in the N_{fail_i} parameter family for each load block, resulting from the uncertainty within σ_{MAX_i}, σ_{MIN_i} and σ_{UTS}, within the Fatigue Damage Model without violating the uncertainty independence assumption. This was achieved by pseudo-randomly sampling values for σ_{MAX_i}, σ_{MIN_i} and σ_{UTS} and evaluating the N_{fail_i} log-normal distribution parameters μ and σ^{LN} using ***Equations 1-3*** and the curve fits from ***Fig. 9*** and ***10*** across 500 iterations for each load block. The mean of the resulting μ and σ^{LN} values were then evaluated, producing updated N_{fail_i} probability distribution parameters. The updated distributions were then used as the distributions for the N_{fail_i} family within the Fatigue Damage Model and example distribution parameters are shown in ***Table 6***. The updated N_{fail_i} distributions showed increased σ^{LN} values and hence increased uncertainty.

Table 6: *Updated N_{fail_i} distribution parameters.*

Load Block	N_{fail_i} μ	N_{fail_i} σ^{LN}	Updated μ	Updated σ^{LN}
5	6.54	0.14	6.49	0.14
10	8.87	0.33	8.96	0.34
15	11.47	0.66	11.61	0.68

3.3. VBSA of the Fatigue Damage Model

This section of the paper presents and discusses the results from applying the SAFE VBSA to the Fatigue Damage Model, in order to apportion the uncertainty in the component safe-life value to the uncertainty in N_{fail_i}, n_i, σ_{FL} and D_{fail} using the main effect sensitivity index. When accounting for the uncertainty within these parameter families, the mean component safe-life value was found to be 27,912 landings, with a variance of 3.74 x 10^7. This shows an increase in the mean safe-life value of 4343 landings when accounting for uncertainty. The minimum safe-life value generated during the VBSA was 7,979 landings. This value is a factor of 3.5 smaller than the mean safe-life value and therefore is reflective of the reduction factors of 3 to 5 required for component safe-life values [8].

The ranking of parameters with respect to their individual contribution to the uncertainty in the safe-life value resulting from the VBSA is shown in ***Table 7. Table 7*** also shows the main effect S_I value, along with the normalised percentage contribution towards the uncertainty in the component safe-life value for each parameter of the Fatigue Damage Model. The parameter which contributes most to the output uncertainty for each parameter family (N_{fail_i}, n_i, σ_{FL} and D_{fail}) is shown in bold.

Table 7: *Fatigue Damage Model VBSA Parameter Ranking.*

Parameter Ranking	Parameter	S_I	% Uncertainty Contribution
1	$\boldsymbol{N_{fail_{15}}}$	**0.575**	**57.49 %**
2	$\boldsymbol{n_{15}}$	**0.167**	**16.73 %**
3	$\boldsymbol{D_{fail}}$	**0.088**	**8.77 %**
4	n_8	0.053	5.27 %
5	$N_{fail_{10}}$	0.018	1.77 %
6	n_{10}	0.018	1.77 %
7	n_2	0.017	1.68 %
8	N_{fail_2}	0.015	1.45 %
9	n_6	0.014	1.42 %
10	$N_{fail_{11}}$	0.012	1.18 %
11	$N_{fail_{14}}$	0.011	1.11 %
12	n_{13}	0.009	0.86 %
13	n_4	0.007	0.70 %
14	n_5	0.007	0.66 %
15	n_9	0.006	0.62 %
16	n_3	0.006	0.62 %
17	n_{12}	0.005	0.54 %
18	$N_{fail_{13}}$	0.005	0.54 %
19	N_{fail_9}	0.004	0.39 %
20	N_{fail_4}	0.004	0.39 %
21	n_1	0.004	0.37 %
22	$N_{fail_{16}}$	0.002	0.24 %
23	N_{fail_3}	0.002	0.22 %
24	n_{16}	0.002	0.21 %
25	n_{18}	0.002	0.20 %
26	n_{17}	0.002	0.20 %
27	$N_{fail_{17}}$	0.002	0.20 %
28	$N_{fail_{18}}$	0.002	0.20 %
29	$\boldsymbol{\sigma_{FL}}$	**0.002**	**0.20 %**
30	N_{fail_5}	0.002	0.19 %
31	N_{fail_6}	0.002	0.19 %
32	n_{14}	0.002	0.18 %
33	N_{fail_7}	0.002	0.17 %
34	N_{fail_1}	0.002	0.17 %
35	N_{fail_8}	0.002	0.15 %
36	$N_{fail_{12}}$	0.001	0.12 %
37	n_{11}	0.000	0.03 %
38	n_7	0.000	0.02 %

As can be seen in ***Table 7***, the number of cycles to cause failure for Load Block 15 ($N_{fail_{15}}$) provided the largest contribution to the uncertainty in the safe-life value of the landing gear component with S_I = 0.575. This corresponds to $N_{fail_{15}}$ contributing to 57.49% of the uncertainty which is exhibited in the component safe-life value. Load block 15 also provided the maximum S_I value for the number of applied load cycles n_{15} parameter with an S_I = 0.167. The third highest uncertainty contribution of 8.77% can be attributed to D_{fail}. By comparison, the uncertainty in the fatigue limit parameter σ_{FL} only contributed to 0.20% of the uncertainty in the component safe-life value. The total uncertainty contributions from the N_{fail_i} and n_i families were 61.7% and 29.9% respectively.

Visualisation techniques form a vital element of Global Sensitivity Analysis (GSA) [20]. However, due to the large number of parameters within the VBSA of the Fatigue Damage Model, the use of 'traditional' sensitivity analysis visualisation methods, such as scatterplots [16], parallel coordinate plots [14] and main effect box plots [14], was impractical as many plots would be required due to the large number of process parameters (i.e. 38 scatterplots would be required). Therefore, an alternative visualisation method was required to represent the parameter ranking in ***Table 7***, such that the parameter ranking could be interpreted in such a manner that enabled the user to compare the contribution to the output uncertainty across the parameter families. In addition, a visualisation method which could distinguish between the small differences between the S_I values was also required.

Therefore, a visualisation method known as 'Parameter Family Visualisation' (PFV) was developed by the authors and is shown in ***Fig. 13***. The purpose of the PFV was to enable the quick and intuitive visualisation of how the S_I values of individual parameters relate to one another, along with displaying how S_I values vary with the 'nominal' value of each parameter (i.e. the mean of each parameter probability distribution) across the parameter family. This was achieved by producing the two subplots (***a*** and ***b***) in ***Fig. 13***, which are to be interpreted in tandem supported by the aligned X-axis scales. The subplots show the individual parameter S_I values plotted with respect to the 'nominal' value for the parameter and each subplot visualises one family. Range bars are also used to show the spread of S_I values for each parameter family to highlight the overlap in S_I values between families. S_I values for D_{fail} and σ_{FL} are also shown, with the nominal values of these parameters being displayed on the right hand Y-axis. The number labels on each data point show the load block number that each parameter is associated with.

The PFV method enabled the quick identification of the parameter which contributes most towards the uncertainty in the component safe-life value as this will be plotted at the maximum S_I value shown on the plot (as highlighted by the range bars). The S_I value for $N_{fail_{15}}$ is shown on the far right of ***subplot b*** at S_I = 0.575. The original parameter ranking from ***Table 7*** can be recovered by moving to the left along ***subplots a*** and ***b*** in ***Fig. 13*** simultaneously and the S_I values for n_{15} and D_{fail} are clearly shown on ***subplot a***. The range bars on ***Fig. 13*** show that the range of S_I values for the N_{fail_i} parameter family completely overlaps and extends beyond the range of S_I values for the n_i parameter family. This extended range reflects the larger overall spread in percentage contribution to the safe-life value uncertainty of the N_{fail_i} family**.** Finally, from ***Fig. 13*** it can be seen that there are a large number of parameters, including σ_{FL}, which have very low S_I values

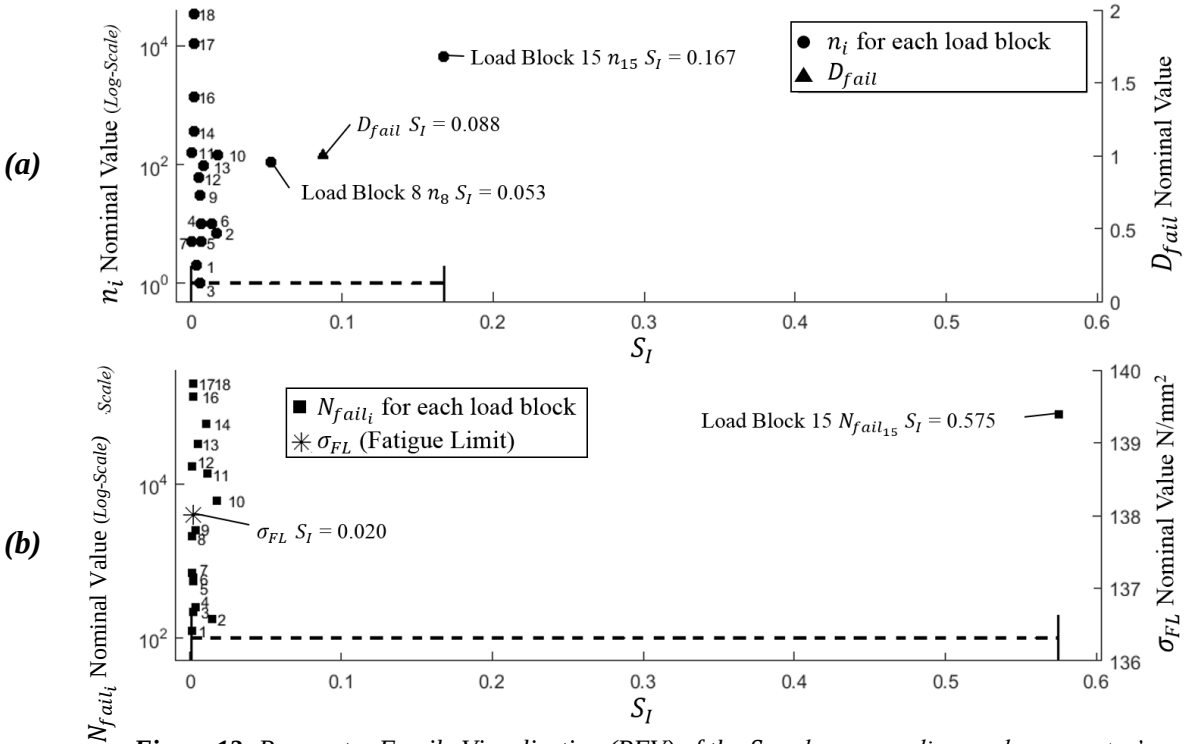

Figure 13: *Parameter Family Visualisation (PFV) of the S_I values regarding each parameter's contribution to the uncertainty in the component safe-life.*

(below 0.005) and these are all clustered to the left hand side of each sub-plot. This clustering shows that the uncertainty within the landing gear component safe-life value is due to only a few influential parameters ($N_{fail_{15}}$, n_{15}, and D_{fail}), whilst the remaining parameters within the fatigue damage model have a negligible effect on the component safe-life value uncertainty.

The parameter ranking demonstrated by the VBSA and PFV can be supported by considering the nature of the Fatigue Damage Model. As shown in ***Fig. 13,*** the two parameters which provide the greatest contribution to the uncertainty in the safe-life value, $N_{fail_{15}}$ and n_{15} are both associated with Load Block 15 of the landing gear fatigue spectrum. From applying Miner's Rule (***Equation 4***), Load Block 15 was found to be the load block within the spectrum which accumulated the most fatigue damage within the component, providing 24.6% of the fatigue damage accumulated per loading cycle. Therefore, any perturbation of the Load Block 15 parameters would have a much greater influence on the component safe-life value in comparison to other load blocks and this occurs due to the linear nature of Miner's Rule. This observation validates the VBSA ranking positions of $N_{fail_{15}}$ and n_{15} compared to the other load block related parameters. In addition, the n_{15} log-normal distribution contains a smaller variance (σ^{LN} = 0.30) compared to the $N_{fail_{15}}$ log-normal distribution variance (σ^{LN} = 0.68). Therefore, it would be expected that the greater amount of uncertainty in $N_{fail_{15}}$ would provide a greater contribution to the safe-life value uncertainty than the uncertainty in n_{15}, further supporting the final parameter ranking. Whilst the supporting considerations of the effect of parameter perturbations and relative magnitude of variance can be used to rank the parameters qualitatively and therefore validate the SAFE ranking, VBSA was still required to quantify the uncertainty contributions of each individual parameter. In addition, VBSA provided the ranking positions of D_{fail} and σ_{FL} along with demonstrating that the vast majority of parameters within the process provide a negligible contribution to the uncertainty within the component safe-life value. Generalising the VBSA study results suggests that in order to reduce the current conservatism required within the safe-life design process, future work should be focused on reducing the uncertainty in the number of cycles to failure and number of applied cycles associated with the load block which accumulates the most fatigue damage within the component. This could be achieved through increased material coupon testing and further measurements of in-service loads [38].

3.4. Validation of the Fatigue Damage Model Parameter Ranking

In order to validate the parameter ranking produced by the SAFE toolbox, an alternative approximate method was used to evaluate the main effect sensitivity index S_I [16]. This alternative method uses a Monte Carlo simulation (MCS), in which the process model is evaluated over many iterations, each time taking new samples from the input parameter probability distributions [16]. For each parameter, the output values from the MCS are arranged in order of increasing input parameter value. The ordered output values are then split into 'bins', within which the mean value of the output is calculated [16]. The variance of the output mean is then calculated across each of the bins and this provides an approximation of the numerator of the main effect sensitivity index S_I. To compute this for the Fatigue Damage Model, 50,000 pseudo-random samples (and hence model evaluations) for each parameter were required to ensure that the sampled values were representative of their source probability distributions.

The SAFE toolbox parameter ranking was found to be in agreement with first three entries of the validation ranking, which computed the S_I for $N_{fail_{15}}$, n_{15} and D_{fail} to be S_I = 0.534, S_I = 0.104 and S_I = 0.083 respectively. However, it was found that the remainder of the validation ranking was not in agreement with the SAFE ranking. This is as a result of the stochastic basis of each method for evaluating the sensitivity index, coupled with the small differences between S_I values of the parameters which provide a negligible contribution to the safe-life value uncertainty. Due to the small difference between S_I values, it would only require a slight variation in the sampled parameter values to alter the parameter ranking. As VBSA methods are essentially stochastic due to their reliance on sampling, this has resulted in the differing parameter rankings for the two methods. However, this does not present a concern as both methods identified the same influential parameters, as well as identifying the group of parameters which only provided a negligible contribution to the output uncertainty (i.e. non-influential parameters were not shown to be influential). To further support the validation, the percentage contribution to the safe-life value uncertainty for complete parameter families was computed for the validation method and are shown in ***Table 8.*** It can be seen that there is good agreement between the percentage contributions from SAFE and the validation method.

Table 8: *Comparison of SAFE and Validation VBSA parameter family contributions.*

Parameter Family	SAFE Toolbox % Contribution	Validation Method % Contribution [16]
N_{fail_i}	61.7	60.6
n_i	29.9	26.6

3.5. VBSA of the 300M SN Model

The SAFE toolbox was also used to conduct VBSA on the 300M SN Model in order to apportion the uncertainty in the 'updated' number of cycles to failure N_{fail_i} parameter family to the uncertainty in the stress parameters σ_{MAX_i}, σ_{MIN_i} and σ_{UTS}. Due to the large number of load blocks and its significant contribution to the safe-life value uncertainty, only $N_{fail_{15}}$ for Load Block 15 was evaluated. The decomposition of the uncertainty in the 'updated' N_{fail_i} distributions was achieved by considering the

increase in the variance of the updated $N_{fail_{15}}$ distribution from the 300M SN Model. It should be noted that the uncertainty in N_{fail_i} is also composed of the original 300M SN data scatter. It can be seen in ***Table 9*** that accounting for the uncertainty in $\sigma_{MAX_{15}}$, $\sigma_{MIN_{15}}$ and σ_{UTS} using the 300M SN Model resulted in an increase in the $N_{fail_{15}}$ distribution variance by a factor of 1.44. This corresponds to the original variance in $N_{fail_{15}}$ from the SN data scatter contributing to 69.3% of the variance and hence uncertainty in the updated $N_{fail_{15}}$ distribution.

Table 9: *$N_{fail_{15}}$ SN data and updated distributions.*

Distribution	Distribution Mean	Distribution Variance
SN data $N_{fail_{15}}$	1.193 x 10^5	7.739 x 10^9
Updated $N_{fail_{15}}$	1.386 x 10^5	1.115 x 10^{10}

The remaining 30.7% of the variance in the updated $N_{fail_{15}}$ distribution was then apportioned to the uncertainty in the Load Block 15 stress levels ($\sigma_{MAX_{15}}$, $\sigma_{MIN_{15}}$) and the 300M σ_{UTS}. This was achieved by applying the SAFE toolbox VBSA to the curve fit used to calculate the log-normal σ^{LN} parameter for the updated $N_{fail_{15}}$ distribution in order to compute the parameter main effect indices. The resulting S_I values are shown in the parameter ranking in ***Table 10.*** These S_I values can be used as a proxy for the percentage contribution to the increase in the variance of the updated $N_{fail_{15}}$ distribution. These percentage contribution values were then applied to the 30.7% variance contribution of the three stress parameters, in order to identify the percentage contribution of each parameter to the $N_{fail_{15}}$ distribution variance increase. These are also shown in ***Table 10***.

Table 10: *Parameter ranking resulting from VBSA of the 300M SN model.*

Parameter	S_I (from 300M SN VBSA)	% Contribution to $N_{fail_{15}}$ Variance
SN Data Scatter	-	69.3 %
$\sigma_{MIN_{15}}$	0.215	21.3 %
$\sigma_{MAX_{15}}$	0.674	6.5 %
σ_{UTS}	0.112	2.9 %

From ***Table 10*** it can be seen that the original scatter in the SN data contributes the most to the uncertainty within the updated $N_{fail_{15}}$ parameter, whilst $\sigma_{MIN_{15}}$, $\sigma_{MAX_{15}}$ and σ_{UTS} provide a contribution of 21.3%, 6.5% and 2.9% respectively. The stress parameter ranking can be qualitatively supported by considering the uncertainty present within the $\sigma_{MIN_{15}}$, $\sigma_{MAX_{15}}$ and σ_{UTS} parameters. The potential stress level range (shown in ***Table 2***) for $\sigma_{MIN_{15}}$ is 148 N/mm^2 compared to the smaller range for $\sigma_{MAX_{15}}$ of 21 N/mm^2. Therefore, the $\sigma_{MIN_{15}}$ contains a greater amount of uncertainty than the $\sigma_{MAX_{15}}$ parameter and hence would provide a greater contribution to the increase in the variance of the updated $N_{fail_{15}}$ distribution. However, the σ_{UTS} ranking position had to be established using VBSA as it is represented by a Gaussian distribution rather than a uniform distribution and therefore the equivalent 'range' argument cannot be applied. Whilst S_I values apportioned the uncertainty within the $N_{fail_{15}}$ parameter to the $\sigma_{MIN_{15}}$, $\sigma_{MAX_{15}}$ and σ_{UTS} parameters, the contribution of the σ_{MAX_i}, σ_{MIN_i} and σ_{UTS} families to the uncertainty in the component safe-life value using S_I values could not be evaluated due to the uncertainty independence assumption. Therefore, no reliable observations can be drawn about how the component safe-life value uncertainty is impacted by the uncertainty in the three stress parameters from this study.

3.6. Feasibility of Applying VBSA Methods to the Safe-Life Fatigue Design Process

Following the application of the SAFE toolbox to implement VBSA on the Fatigue Damage Model and 300M SN Model, the feasibility of applying VBSA methods to further work regarding the investigation of the uncertainty within the safe-life fatigue design process can be discussed. The results presented in this paper have shown that the main effect sensitivity index VBSA method can be used to generate a ranking of the parameters within the process with respect to their contribution to the uncertainty in the landing gear component safe-life value. The parameter ranking identified that the number of cycles to failure for the load block which was most damaging to the component provided the majority of the uncertainty in the component safe-life value. An additional outcome was that the parameter ranking in conjunction with the PFV method highlighted that a significant number of the parameters within the process provided a negligible contribution to the safe-life value uncertainty. This means in future studies, these parameters could be fixed to 'nominal' values, which is known as parameter 'screening' [14] [16]. The benefit arising from these two outcomes is a reduction in the resources required to conduct further studies, as future work can be targeted at the specific parameters which provide the largest contribution to the process uncertainty [14]. These further studies would be conducted with the aim of investigating and reducing the uncertainty in the targeted parameters in order to challenge the conservatism required within the safe-life fatigue design process.

Despite these results showing a successful outcome for applying the over-arching concept of VBSA to the safe-life fatigue design process, there are limitations to the specific method implemented within this paper. These limitations restrict the feasibility of applying the SAFE toolbox main effect sensitivity index VBSA method to future work.

Firstly, the need to de-couple the dependency between the uncertainty in the N_{fail_i} parameters and the stress parameter families σ_{MAX_i}, σ_{MIN_i} and σ_{UTS} prevented the computation of S_I values for all 75 parameters within the safe-life design process model. This was because the SAFE toolbox main effect index estimator was unable to apportion the uncertainty within the safe-life value directly to the uncertainty within the σ_{MAX_i}, σ_{MIN_i} and σ_{UTS}

parameter families and therefore, could only apportion the uncertainty in the $N_{fail_{15}}$ parameter to these three parameter families. Therefore, estimators and sampling strategies which can account for dependency between parameter uncertainties should be implemented instead to remove the need to de-couple the safe-life fatigue design process model. Such estimators have been proposed within the literature [45] [46] and the implementation of these estimators would enable VBSA of the complete process, considering the impact of uncertainty in the stress parameter families σ_{MAX_i}, σ_{MIN_i} and σ_{UTS} of each load block. It should be noted that the infeasibility of applying the SAFE toolbox main effect sensitivity index estimator within future work is as a result of the nature of the safe-life fatigue design process violating the uncertainty independence assumption used within the estimator and not as a result of the toolbox itself. The SAFE toolbox was found to be a comprehensive GSA toolbox which integrated effortlessly into the Fatigue Damage Model and 300M SN Model, especially considering the inbuilt sampling functions. Considering future application of the toolbox, Total Effect indices will be required to verify that parameters shown to be suitable for screening remain so when accounting for parameter interactions [14]. Other GSA methods from the literature, such as the Fourier Amplitude Sensitivity Testing (FAST) method [13], should be evaluated for their suitability for use in this application.

The estimator used for the main effect sensitivity index also proved to be computationally expensive. Whilst only 3,000 samples were required from each parameter probability distribution to achieve repeatable parameter rankings, this resulted in 57,000 model evaluations being required to generate the parameter ranking. The large number of model evaluations is as a result of the large number of parameters within the Fatigue Damage Model, and this can be highlighted by considering the 300M SN Model which required only 1,500 model evaluations due to having only 3 parameters. The approximate validation method required 50,000 model evaluations using 50,000 samples for each parameter. Due to the analytical nature of the Fatigue Damage Model, the large number of model iterations did not present a challenge when implementing the estimator. However, if there was the need to convert a load spectrum into component stresses using a finite element model, as is commonly performed in industry [32], the high number of model evaluations and analysis run time required could become prohibitive. This could require the use of surrogate models or emulators to reduce run time [14].

The other challenge presented by the large number of uncertain parameters is regarding the visualisation of the VBSA results and parameter ranking as it is not feasible to 'scale-up' traditional visualisation methods to the large number of parameters contained within the safe-life fatigue design process. However, the development of visualisation methods, such as the PFV, will support the intuitive understanding of the results of VBSA on processes with large numbers of uncertain parameters. Therefore, the visualisation of VBSA results does not pose a risk to the feasibility of applying VBSA methods within future work. In addition, by plotting the nominal value for the parameter against the parameter S_I value, the PFV will be able to visualise trends that may develop regarding parameter family uncertainty contributions. For example if the S_I value of a parameter family increased with the parameter nominal value, the PFV would show this trend.

4. CONCLUSION

This paper has presented the application of VBSA methods to the safe-life fatigue design process of a hypothetical landing gear component using the SAFE toolbox. The results of the VBSA in conjunction with a novel visualisation method showed that the parameter representing the number of cycles to cause failure which is associated with the load block that accumulated the most fatigue damage within the component provided the greatest contribution to the uncertainty in the component safe-life value. In addition, the majority of the parameters within the process, including the material fatigue limit, were shown to have a negligible effect on the uncertainty within the component safe-life value. Therefore, the VBSA results also enabled parameter 'screening' and these parameters could be fixed to 'nominal' values within further studies.

Whilst the overarching concept of VBSA methods has been shown to be suitable for generating a parameter ranking for the safe-life process, the specific method implemented within this study showed limitations due to the large number of parameters and dependency which exists between parameter uncertainties within the safe-life design process. VBSA estimators and global sensitivity analysis methods which can account for uncertainty dependency between parameters have been identified in the literature and should be applied within future work. In addition, the safe-life fatigue design process model should be modified to better reflect current industrial practice, such as the use of finite element programs to evaluate component stresses. The development of emulators and surrogate models for use with the more complex process model is also intended.

Considering the wider contribution to the safe-life fatigue design field, this paper has shown that VBSA methods provide a route to identifying the elements of the design process which contribute the most towards the uncertainty within component safe-life values. Therefore, the insight provided by further detailed VBSA studies could enable engineers to understand the uncertainty currently present within the design process in order to focus future research on challenging the conservatism required for component safe-life values. In addition, future work will also contribute to the global sensitivity analysis field, through the implementation and development of state-of-the-art sensitivity analysis and visualisation methods.

ACKNOWLEDGEMENTS

The authors would like to thank the University of Bristol Alumni Foundation for assistance with conference fees. The authors would also like to thank the developers of the SAFE Toolbox.

REFERENCES

[1] Boller, C., et al. *Encyclopaedia of Structural Health Monitoring*, 2009, John Wiley & Sons Ltd. ISBN: 978-0-470-05822-0.

[2] *Landing Gear Design Loads, ARGARD Conference Proceedings 484* report no. AGARD-CP-484, Advisory Group for Aerospace Research and Development, France, 1991, 50-60.

[3] Braga, D., et al. *Advanced design for lightweight structures: Review and prospects*. Progress in Aerospace Sciences 2014, 69, 29-39.

[4] Lombardo, D. C., Fraser, K. F. *Importance of Reliability Assessment to Helicopter Structural Component Fatigue Life Prediction*, report no. DSTO-TON-0462, DSTO Aeronautical and Maritime Research Laboratory, Australia, 2002.

[5] Dilger, R., et al. *Eurofighter a safe life aircraft in the age of damage tolerance*. Intl. Journal of Fatigue 2009, 31, 1017-1023.

[6] *CS-29 Book 1 Certification Specifications for Large Rotorcraft Amendment 3*, European Aviation Safety Agency (EASA)

[7] Fatemi, A., Yang, L. *Cumulative fatigue damage and life prediction theories: a survey of the state of the art for homogenous materials*. Intl. Journal of Fatigue 1998, 20, 1, 9-34.

[8] *CS-25 Book 2 Acceptable Means of Compliance*, EASA Certification Specifications for Large Aeroplanes.

[9] *DEF STAN 00-970 Part 1 Section 3 Leaflet 35 Fatigue Safe Life Substantiation*. UK MOD.

[10] Iyyer, N., et al. *Aircraft life management using crack initiation and crack growth models – P-3C Aircraft Experience*. Intl. Journal of Fatigue, 2007, 29, 1584-1607.

[11] Cavallini., G., Lazzeri, R. *A probabilistic approach to fatigue risk assessment in aerospace components*, Engineering Fracture Mechanics, 2007, 74, 2964-2970.

[12] Bagnoli, F., et al. *Fatigue fracture of a main landing gear swinging lever in a civil aircraft*. Eng. Failure Analysis, 2008, 15, 755-765.

[13] Iooss, B., Lemaître, P. *A review of global sensitivity analysis methods*. Chapter of Meloni, C., Dellino, G. *Uncertainty Management in Simulation-Optimization of Complex Systems: Algorithms and Applications*, 2015, Springer, ISBN: 978-1-4899-7546-1.

[14] Pianosi, F., et al. *Sensitivity Analysis of environmental models: A systematic review with practical workflow*. Environmental Modelling & Software, 2016, 79, 214-232.

[15] Chan, K., et al. *Sensitivity Analysis of Model Output: Variance-Based Methods Make the Difference*, Proceedings of the 1997 Winter Simulation Conference (Eds. Andradóttir, S. et al), Atlanta, Georgia, USA, 7-10 December 1997.

[16] Saltelli, A., et al. *Global Sensitivity Analysis: The Primer*, 2008, John Wiley & Sons Ltd. ISBN: 978-0-470-05997-5.

[17] Cannavó, F. *Sensitivity analysis for volcanic source modelling quality assessment and model selection*. Computers & Geosciences, 2012, 44, 52-59.

[18] Quaglietta, E., Punzo, V. *Supporting the design of railway systems by means of Sobal variance-based sensitivity analysis*. Transportation Research Part C, 2013, 34, 38-54.

[19] Brevault, L., et al. *Comparison of different global sensitivity analysis methods for aerospace vehicle optimal design.* 10th World Congress on Structural and Multidisciplinary Optimization, Orlando, Florida, USA, 19-24 May 2013.

[20] Pianosi, F., et al. *A Matlab toolbox for Global Sensitivity Analysis*. Environmental Modelling & Software, 2015, 70, 80-85.

[21] MATLAB version 8.5.1 Natik, Massachusetts: The MathWorks Inc., 2014.

[22] McFarland, M., Riha, D. *Uncertainty Quantification Methods for Helicopter Fatigue Reliability Analysis*. American Helicopter Society 65th Annual Forum, Texas, USA, 27-29 May 2009.

[23] Paolino, D., Cavatorta, M. *On the application of the stochastic approach in predicting fatigue reliability using Miner's damage rule*. Fatigue & Fracture of Engineering Materials and Structures, 2013, 37, 107-117.

[24] Shen, H., et al. *Probabilistic model on stochastic fatigue damage*. Intl. Journal of Fatigue, 2000, 22, 569-572.

[25] Sun, Q., et al. *A statistically consistent fatigue damage model based on Miner's Rule*. Intl. Journal of Fatigue, 2014, 69, 16-21.

[26] Popelin, A., Iooss, B. *Visualisation tools for uncertainty and sensitivity analyses on thermal-hydraulic transients*. Joint International Conference on Supercomputing in Nuclear Applications and Monte Carlo, Paris, France, 27-31 October, 2013.

[27] Chan, Y. *The Generalized Sensitivity Scatterplot*. IEEE Transactions on Visualization and Computer Graphics, 2013, 19, 1768-1781.

[28] Liard, F., et al. *Helicopter Fatigue Design Guide*, report no. AGARD-AG-292, Advisory Group for Aerospace Research and Development, France, 1983, 109-130.

[29] *Endurance of high-strength steels data item*, ESDU 04019a, Engineering Sciences Data Unit, United Kingdom, 2004, 42,43.

[30] *Standard fatigue loading sequences*, ESDU 97018, Engineering Sciences Data Unit, United Kingdom, 2003.

[31] Potter, J. M., Watanabe, R. T. *Development of Fatigue Loading Spectra*, ASTM special technical publication Volume 1006, ASTM, 1989, ISBN: 978-0-08-0311185-1.

[32] Sartor, P., et al. *Bayesian sensitivity analysis of flight parameters that affect main landing gear yield locations*. The Aeronautical Journal, 2014, 118, 1210, 1481-1497.

[33] Boardman, B., et al. *Fatigue Resistance of Steels*, ASM Handbook, Volume 1: Properties and Selection: Irons, Steels, and High-Performance Alloys, ASM International, 1990, 673-688.

[34] Currey, N. S. *Aircraft Landing Gear Design: Principles and Practices.* AIAA Education Series, AIAA, 1988, ISBN: 978-1-6008-6018-8.

[35] *Metallic Materials and Elements for Aerospace Vehicle Structures*, report no. MIL-HDBK-5H, Department of Defense, United States of America, 1998, 2-10 to 2-66.

[36] Saff, C. R., Rosenfeld, M. S., *Load-Environment Interaction Effects on Crack Growth in Landing Gear Steels***,** Chapter from *Design of Fatigue and Fracture Resistant Structures* (Eds. Abelkis, P. R., Hudson, C. M.), ASTM Special Technical Publication 761, ASTM, 1982.

[37] Weibel, J. P. *Undercarriage Loadings of Three Aircraft: Porter PC-6, Venom DH-112 and Mirage IIIS*. Proceedings of Aircraft Fatigue: Design, Operational and Economic Aspects Symposium (Eds. Mann, J. Y., Milligan, I.), Melbourne, Australia, 22-24 May 1967, Pergamon Press (Australia) Pty Limited, SBN: 08-017526-0.

[38] Lombardo, D. C. *Helicopter Structures – A review of loads, fatigue design techniques and usage monitoring*, report no. AR-007-137, Department of Defence, Defence Science and Technology Organisation, Aeronautical Research Laboratory, Australia, 1993.

[39] Bright, G. W., et al. *Variability in the mechanical properties and processing conditions of High Strength Low Alloy steels*, Procedia Engineering, 2011, 10, 106-111.

[40] Osgood, C. *Fatigue Design*, 1970, Wiley-Interscience, ISBN: 0417657115.

[41] Saltelli, A., et al, *Variance based sensitivity analysis of model output. Design and estimator for the total sensitivity index*. Computer Physics Communications, 2010, 181, 259-270.

[42] Helton, J. C., Davis, F. J. *Latin hypercube sampling and propagation of uncertainty in analyses of complex systems*. Reliability Engineering and System Safety, 2003, 81, 23-69.

[43] Swiler, L. P., et al. *Epistemic Uncertainty Quantification Tutorial*, Proceedings of the IMAC-XXVII, Society for Experimental Mechanics Inc. , Orlando, Florida, USA, 9-12 February 2009.

[44] Buch, A. *The damage sum in fatigue of structure components.* Engineering Fracture Mechanics, 1978, 10, 233-247.

[45] Saltelli, A., Trantola, S. *On the Relative Importance of Input Factors in Mathematical Models: Safety Assessment for Nuclear Waste Disposal*. Journal of the American Statistical Association, 2002, 97, 702-709.

[46] Borgonovo, E., Tarantola, S. *Moment independent and variance-based sensitivity analysis with correlations.* An application to the stability of a chemical reactor. Int. Journal of Chemical Kinetics, 2008, 40, 687-698.